Visual Neuroscience (2008), **25**, 301–306. Printed in the USA.

doi:10.1017/S0952523808080474

Topography of the long- to middle-wavelength sensitive cone ratio in the human retina assessed with a wide-field color multifocal electroretinogram

JAMES A. KUCHENBECKER, MANISHA SAHAY, DIANE M. TAIT, MAUREEN NEITZ, AND JAY NEITZ

Department of Ophthalmology, and Department of Cell Biology, Neurobiology & Anatomy, Medical College of Wisconsin, Milwaukee, Wisconsin

(RECEIVED October 22, 2007; ACCEPTED February 27, 2008)

Abstract

The topographical distribution of relative sensitivity to red and green lights across the retina was assayed using a custom-made wide-field color multifocal electroretinogram apparatus. There were increases in the relative sensitivity to red compared to green light in the periphery that correlate with observed increases in the relative amount of long (L) compared to middle (M) wavelength sensitive opsin mRNA. These results provide electrophysiological evidence that there is a dramatic increase in the ratio of L to M cones in the far periphery of the human retina. The central to far peripheral homogeneity in cone proportions has implications for understanding the developmental mechanisms that determine the identity of a cone as L or M and for understanding the circuitry for color vision in the peripheral retina.

Keywords: Cone photopigments, Cone topography, Cone photo pigment gene expression, Multifocal electroretinogram

Introduction

The numbers and distributions of all three classes of cone photoreceptors in the central retina of the living human eye can be visualized using adaptive optics imaging coupled with retinal densitometry (Roorda & Williams, 1999; Roorda et al., 2001; Hofer et al., 2005). However, adaptive optics has not yet allowed imaging of the chromatic topography of the retina for eccentricities greater than approximately 8°. The high degree of similarity of the opsins has obviated separate mapping of L and M cones using antibody staining or in situ hybridization. However, previous studies have demonstrated that the analysis of L versus M opsin messenger RNA (mRNA) using reverse transcriptase and the polymerase chain reaction is an effective method for estimating the relative L:M cone ratio at specific retinal locations (Hagstrom et al., 1998, 2000; Deeb et al., 2000; Bollinger et al., 2004). In humans, the relative ratio of L versus M opsin mRNA has been observed to vary as a function of retinal location and it has been reported that there is a dramatic increase in the relative amount of L opsin mRNA at eccentricities greater than about 40° (Hagstrom et al., 1998, 2000; Neitz et al., 2006). To the extent that peripheral mRNA ratios reflect cone ratios, these findings suggest that the relative proportion of M cones approaches zero in the far peripheral human retina. This is consistent with a report from microspectrophotometry measurements in which eight out of nine cones from the far periphery of one human retina were classed as L (Bowmaker et al., 2003).

Other explanations besides a change in cone proportions with eccentricity might be forwarded for the differences in mRNA ratio between central and far peripheral retina, although they seem unlikely. For example, one could speculate that unlike the L and M cones in the central retina those in the far periphery express or turnover mRNA unequally. The electroretinogram (ERG) has been an effective tool for investigating cone-derived signals in the retina (Hood et al., 2002; Murray et al., 2004) and has recently been proven to accurately predict relative differences in L:M cone ratio across individual in a direct comparison with results in the central retina from adaptive optics imaging (Hofer et al., 2005). However, the putative cone ratio changes that are suggested by the mRNA results are most dramatic in the far periphery beyond 40° of eccentricity with the percentage of cones approaching 100% L near the ora serrata. Stimulation of the far peripheral retina has not been possible with a Maxwellian view system as has been used to obtain ERG flicker spectral sensitivity for estimating cone ratios (Jacobs et al., 1996) nor have responses beyond 40° from the fovea been obtained with cone isolating multifocal- (mf-) ERG (Albrecht et al., 2002) using a cathode ray tube stimulator. Here, to measure

Address correspondence and reprint requests to: Jay Neitz, Department of Ophthalmology, The Eye Institute, 925 North 87th Street, Milwaukee, WI 53226-4812. E-mail: jneitz@mcw.edu

relative sensitivity to middle and long wavelength lights in the far periphery, red (650 nm) and green (527 nm) super bright light emitting diodes (LEDs) were used as light sources in a new wide-field hemispherically shaped stimulator of our own construction to obtain wide field color mf-ERGs subtending 150° of visual angle. We report relative sensitivity to red light increases in the far peripheral retina exactly as expected if the L to M cone proportion approaches one for far eccentric retina locations.

Materials and methods

Subjects

Three deuteranopes, one protanope, and four-color normal trichromats participated in the study. Color vision status was confirmed by Nagel anomaloscope and by a battery of standard color vision tests.

mf-ERG description

Control signals from a clinical mf-ERG system from Roland Consult (DE 147770 Brandenburg, Germany HRB 8835, VAT DE 176754912) were re-routed and modified for use with a custom-made color LED stimulator. One of the major design goals of the new stimulus was to be able to obtain a robust signal from cone photoreceptors out in the far periphery (greater than 70° from fovea). Consequently, several features were incorporated aimed at improving signal-to-noise ratio (SNR) in the far peripheral retina.

Printed circuit boards were trapezoidal shaped so that when placed edge-to-edge they created a geodesic, approximately hemispherical, dome (Fig. 1a). One-thousand-twenty-four pairs of red (650 nm) and green (527 nm) super bright LEDs were spaced uniformly to cover the concave surface of the dome. The wavelengths were chosen to produce a large difference in relative spectral sensitivity between L and M cones and at the same time minimizing short (S) wavelength sensitive cone stimulation with the shorter wavelength LED (Carroll et al., 2000). Each individual LED was aimed to concentrate their energy to a focal point positioned just beyond the center of a theoretical surface formed by the dome. Cyclic summation was chosen to encode/decode region specific information (Lindenberg et al., 2003). In this method, each stimulus field is 50% duty-cycle square-wave modulated at a minimally different frequency. In the measurements

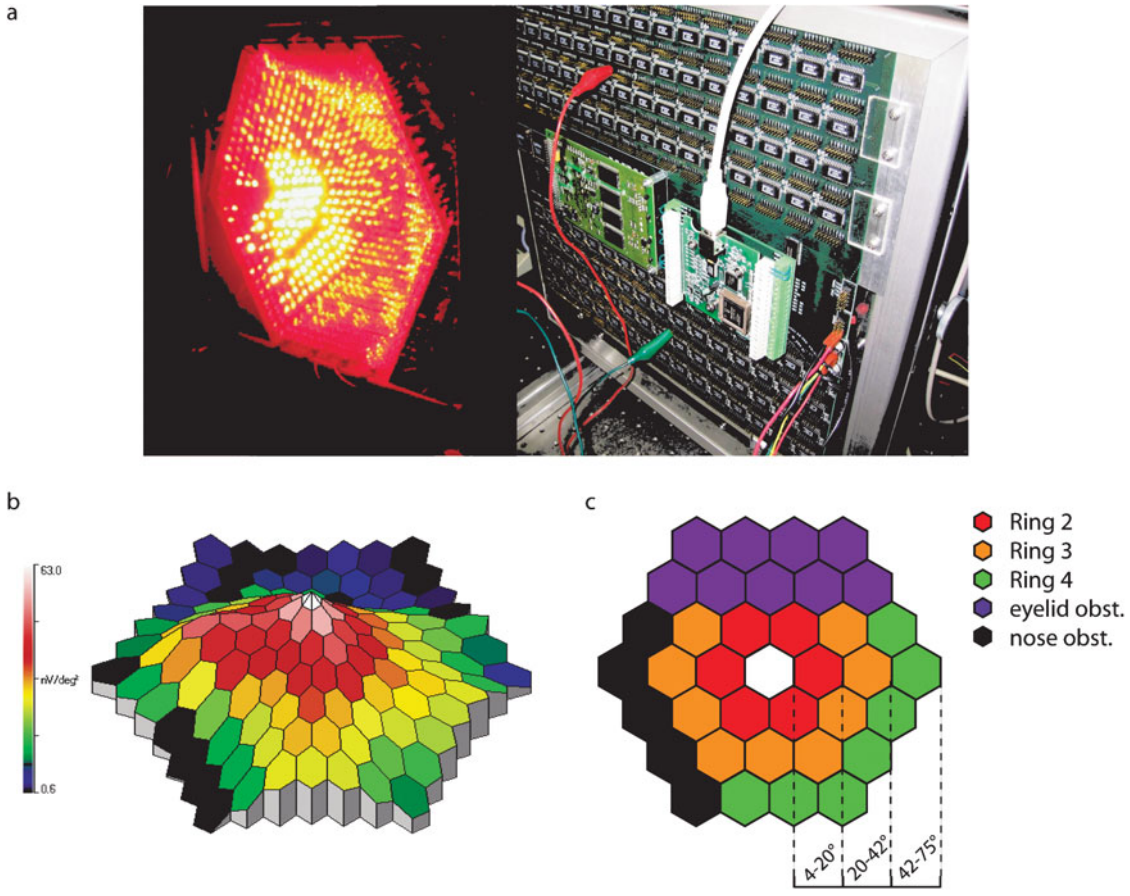

Fig. 1. The mf-ERG hardware, example mf-ERG response profile, and analysis of concentric rings representing different retinal eccentricities. (**a**) The stimulator was designed and constructed out of specially shaped circuit boards so that when placed edge-to-edge created a geodesic dome. Super bright LEDs were then aimed to a focal point and cyclic summation was used to extract topographical regions. The 650 nm LEDs were on in the photograph. (**b**) A typical mf-ERG response profile obtained from the device. (**c**) To compare different retinal eccentricities, ERG amplitudes were averaged from "rings" of increasing eccentricity. Analysis was complicated by the fact that the nose and upper brow obstructed the light entering the eye to a variable extent in different subjects. Unreliable data between trials and subjects were commonly found in these areas. To maintain reliability of collected data, only areas labeled in red, orange, and green were used in the ring averages.

reported here, the nominal stimulus base modulation frequency was 30 Hz. Slight differences in frequency from the base value allowed mathematical separation of region specific responses corresponding to 37 different stimulus segments (Fig. 1c). Specifically, segments operated over the range of 29.25–30.75 Hz with individual segments separated by 0.0405 Hz. Since rods and S-cone responses are disadvantaged at 30 Hz, using this frequency range has the additional benefit of obviating rod and S-cone responses in the received signal (Jacobs et al., 1996).

Steps were taken to control against the non-ideal characteristics of LEDs. Each color of LED used came from the same cast to minimize variation that can occur due to the manufacturing process. LEDs were controlled using an array of constant current drivers (Fig. 1a) and intensity of the LEDs was varied *via* pulse frequency modulation (PFM) to prevent shifts in wavelength associated with changes in LED current (Swanson et al., 1987). The PFM signal operates at higher-than-perceivable frequencies (0.9804–250 kHz) and is introduced by combining it by a digital logic "AND" operation with the ~30 Hz square wave that derives the flicker ERG stimulus.

Experimental protocol

The pupil of the right eye of each subject was dilated by administration of Tropicamide (0.5%) and a Dawson, Trick, and Litzkow electrode was placed on the sclera. Subjects were positioned using a chin cup with the test eye at the focal point of the lights. Intensity response curves were generated for the 527 nm and 650 nm LEDs independently by presenting one hundred percent contrast stimuli, starting at 6 log trolands, presented at successively increasing intensities (in 0.3 log unit steps). The goal in generating two intensity response functions is to find the relative quantal intensities of the 527 nm and 650 nm LEDs needed to create an equal ERG response to the two. The method used here for estimating cone ratio is an extension of ERG flicker photometry (Jacobs et al., 1996; Carroll et al., 2000) which makes the assumption that L and M cone signals combine additively in the 30 Hz ERG signal. This assumption has been validated by comparison of relative cone ratio estimates obtained with the flicker ERG to cone ratios directly visualized in the same subjects using adaptive optics imaging (Hofer et al., 2005). Since the relevant variable is the relative quantal catch for two spectrally different lights equated to produce the same ERG response, non-linearities in the intensity response function including those that result from adaptation to the increasingly brighter test lights (Valeton, 1983; Valeton & van Norren, 1983; Kremers et al., 2003) do not influence the result.

Each measurement provided flicker ERG amplitude responses at 37 retinal locations illustrated in Fig. 1c. ERG amplitudes as a function of retinal eccentricity were obtained by averaging the responses for rings at three eccentricities (ring 2 spans ~4–20°, ring 3 spans ~20–42°, and ring 4 spans ~42–75°) shown in Fig. 1c. The segment corresponding to stimulation of the fovea was not used in these analyses to avoid confounds that could arise from contributions of macular pigment and variations in photopigment optical density in the fovea. Subjects' noses and orbital ridges obstructed the stimuli to a variable extent producing unreliable results across subjects in the lower left and upper quadrants respectively; consequently, these areas were excluded in the ring analysis as indicated in Fig. 1c.

Intensity response data were best fit to sigmoidal curves described by an integrated Gaussian function where the mean, standard deviation, and maximum were adjusted to minimize error using Newton's method. Our purpose in fitting the intensity response functions was to provide an objective determination of the relative displacement along the x-axis as a measure of the relative sensitivity to the 527 nm versus 650 nm LEDs. The response to the 527 nm LEDs was fit first by changing three parameters that, respectively, determine the maximum asymptote, the slope of the function in its approximately linear portion and its position on the x-axis. Once this was done, the response to red LEDs was fit by varying only the position of the function on the x-axis, keeping the other parameters constant. The relative sensitivities determined in this manner were compared to values determined by varying the weighted sum of spectral sensitivities to the two lights for the human L and M cones as has been done previously in estimating cone ratios from flicker ERG responses (Carroll et al., 2000). The weights provide a relative estimate of L to M cone contribution to the ERG.

Results

Intensity response functions are shown in Fig. 2. Four color-normal trichromats were tested (Figs. 2c, 2d, 2e, and 2f) with

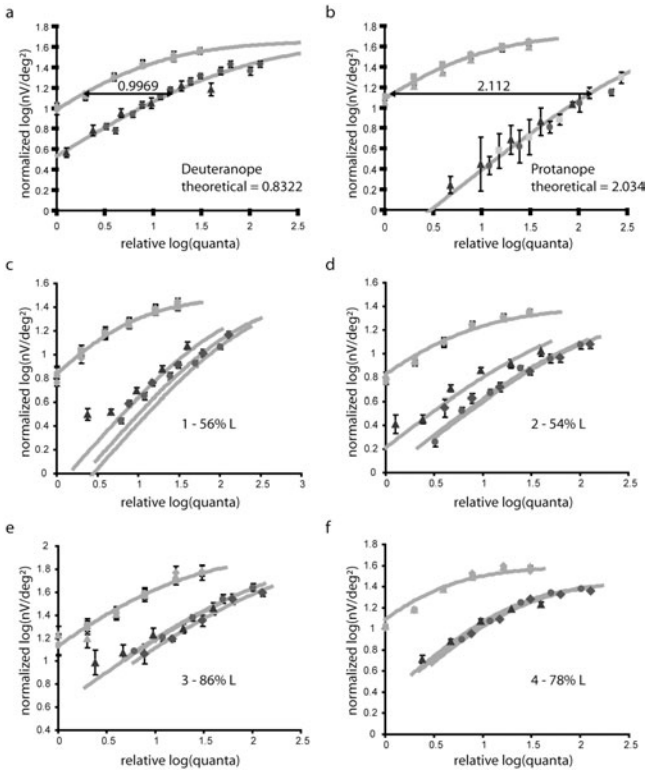

Fig. 2. Intensity response functions obtained with the mf-ERG. Each panel represents 6 conditions. The light colored symbols represent responses to the 527 nm LED and the darker symbols represent responses from the 650 nm LED. Different symbols represent different eccentricities; diamonds, ring 2; filled circles, ring 3; triangles, ring 4. Dichromats were used as controls and served to calibrate the system. (**a**) Average results for four deuteranopes. (**b**) Results for a protanope. Theoretical estimates of sensitivity to the red and green LED wavelengths are in close agreement with measured sensitivity differences for both deuteranopes and protanopes. (**c**, **d**) Subjects JG and JK with low foveal cone ratios showed significant increases in sensitivity to red light as a function of eccentricity. (**e**, **f**) Subjects MM and MP had higher foveal cone ratio and showed little to no increase in sensitivity to red light as a function of eccentricity.

protanopes and deuteranopes serving as controls (Figs. 2a and 2b). Each panel of Fig. 2 displays responses to the green LEDs (leftmost trace) relative to the red LEDs. The amplitudes of the ERG signals monotonically decreased with eccentricity (an example response profile is shown in Fig. 1b). Presumably, part of this decrease is the result of a decrease in photoreceptor density with eccentricity even though the areas of the stimulus segments were increased with eccentricity (as indicated in Fig. 1c) in attempt to compensate for this. Also, even though an attempt was made to take it into account in the measurements of quantal intensity at the different eccentricities, part of the decrease in amplitude must also result from the decreased effective pupil area as light from the periphery enters from an increasingly oblique angle resulting in a ~50% decease in light intensity for ring 4 compared to ring 2.

To compensate for the decrease in ERG amplitude with eccentricity and allow the relative responses between red and green to be more easily appreciated for the different eccentricities, the green LED, rings 2, 3, and 4 (Fig. 1c) are superimposed by translating the responses to both red and green along the y-axis. Thus, the differences in responses for ring 2, 3, and 4 (Fig. 1c) to the red LEDs, reflect changes in relative spectral sensitivity at different retinal eccentricities that can be attributed to changes in cone ratio. ERG response amplitudes are plotted in normalized log nano-volts per square degree (nV/degree^2) versus log relative quantal intensity at the retina. Thus, displacements of the intensity response functions for the red and green lights for the deuteranopes and protanope reflect the relative spectral sensitivities of the L and M cones respectively.

Theoretically, in dichromats, where the responses are determined by a single class of cones, which would not change in spectral sensitivity with eccentricity, the factors that can be used to superimpose the responses to green light at different eccentricities should perfectly superimpose the responses to red. In practice, this did not turn out to be exactly true, especially for the most eccentric ring (ring 4, Fig. 1c). We assume that this is because of some slight differences in the light reaching the retina from the two different colored LEDs, probably because of the optics of the eye itself. To correct for this, the red LED response curves for the deuteranopes were translated a small amount (-0.01 log units from ring 2 to ring 3, and -0.17 log units from ring 2 to ring 4) along the x-axis to superimpose. Once this correction for factors intrinsic to the eye was determined for the deuteranopes, the same correction was applied to the results for the protanopes and the four normal trichromats. With this adjustment, differences in response due to a small differential loss for the red and green lights are eliminated for the far periphery and any residual differences in the intensity response functions can be attributed to changes in the relative contributions of the L and M cones with eccentricity. The validity of this procedure can be seen from the result that same correction used to superimpose the deuteranope results also work for the protanope and nearly superimposes red light responses for normal trichromats with very high L:M ratios (Figs. 2e and 2f) who would not be expected to have large changes in cone ratio with eccentricity (as explained below).

The differences along the x-axis in the curves of Figs. 2a and 2b were 0.9969 log units for the deuteranopes, and 2.112 log units for the protanope. These values are in reasonably good agreement with the sensitivities to both LEDs calculated for dichromats using published L and M spectral absorption curves (Carroll et al., 2000) (predicted differences were 0.8322 and 2.034 log units respectively). These control experiments demonstrate that relative spectral sensitivity can be measured at all eccentricities using this technique with relatively good signal-to-noise ratios. The measurements on dichromats also allowed us to correct for small differences in the amounts of red and green light reaching the retina due to optical factors intrinsic to the eye at different eccentricities that would be impossible to measure otherwise.

Conventional flicker photometric ERGs were performed on the trichromats to obtain an estimate for cone ratio in the central retina (Carroll et al., 2002). From direct comparisons with results from adaptive optics imaging, this method has been shown to accurately reflect foveal cone ratios. Subject 1 was estimated to have 56% L cones, JK 54% L cones, 3 86% L cones, and 4 78% L cones. Sensitivity difference between each ring is shown in Table 1. Subjects 1 and 2 were estimated to have close to equal numbers of L and M cones in the central retina by conventional ERG flicker photometry. Each of them had a significantly smaller difference in spectral sensitivity for the most eccentric ring as predicted if the ratio of L to M cones increases in the periphery (Figs. 2c and 2d). In earlier results from mRNA in cadaver eyes, it was observed that L compared to M mRNA percentages increased to nearly 100% L for all eyes independent of the foveal cone ratio (Neitz et al., 2006). Thus, the change in mRNA ratio was dramatic for individuals with low L cone ratios and very subtle for individuals with high ratios. This predicts that if the mf-ERG is accurately reflecting changes in cone proportions with eccentricity, individuals estimated to have high foveal cone ratios should show little change in relative sensitivity of red to green light with eccentricity. To test this, we ran two subjects estimated to have relatively high foveal L:M cone ratios, 3 and 4, Figs. 2e and 2f. Both had more uniformly high relative sensitivity to red light at all eccentricities.

To evaluate the reliability of the results, data points from intensity response functions for each ring were individually fit to the sigmoidal curves. This process yielded a set of means for each ring that represent the variability in the measurement. For these measurements, analysis of variance was used to determine which differences within each subject were statistically significant. For subject 4, none of the differences between rings was statistically significant. His L:M ratio is high in the central retina so it was predicted that any increases with eccentricity would be small. For all other trichromats (subjects 1, 2, and 3) the difference between ring 2 and 4 was statistically significant (subject 1, $p < 0.05$; subject 2, $p < 0.001$; subject 3, $p < 0.05$). Thus, for all these subjects, there was a highly reliable increase in the relative sensitivity to long wavelength lights for the far periphery compared to the central retina. In addition, for the two subjects with the lowest L:M ratios in the central retina, the differences between rings 3 and 4 were statistically significant (subject 1, $p < 0.01$; subject 2, $p < 0.001$), demonstrating a reliable increase in long-wavelength sensitivity from mid- to far-far periphery. We note that for subject 1 the measured L:M ratio for ring 2 is slightly higher than ring 3, however, this difference was not statistically significant.

Table 1. *Log relative sensitivities to 650 nm and 527 nm LED lights*

	1	2	3	4
ring 2	1.489245	1.498071	1.125247	0.928290
ring 3	1.595114	1.456961	0.973189	0.882337
ring 4	1.294594	1.127281	0.998105	0.848536
foveal L/(L + M)	0.5627	0.5410	0.8593	0.7790

Fig. 3 plots the relative contribution of L and M cones (represented as percent L) in the conventional flicker photometric ERG compared the contribution calculated from the mf-ERG responses at different eccentricities. As expected, there was a good correlation between mf-ERG results and those from flicker photometry for the more central rings (ring 2 and 3) but the results for the most eccentric ring (ring 4) indicated a very large contribution from L cones for all subjects. We note that even for the more central rings the contribution from L cones is higher than that estimated for conventional ERG flicker photometry. Why this technique would favor L cone responses, slightly more than conventional ERG flicker photometry is not clear to us. Nonetheless, the relative changes in sensitivity with eccentricity are consistent with dramatic shifts in L:M cone ratio in the periphery that are pronounced in individuals with low foveal L:M cone ratios.

Discussion

We have used a new LED based wide-field color mf ERG stimulator to assay the relative contributions of L and M cones to the ERG as a function of retinal eccentricity. The technique gives the predicted spectral sensitivities for control dichromats and the results for more central eccentricities are highly correlated with conventional ERG flicker photometry. Subjects with lower foveal cone ratios had relatively larger contributions from L cones to ERG signals generated by the far peripheral retina compared to central retina. These results provide electrophysiological evidence that there is a dramatic increase in the ratio of L to M cones in the far periphery of the human retina.

These results have implications for understanding the mechanisms that determine the identity of L and M cones in the developing primate retina. Differences between S cones and L/M cones indicate that they are indeed different cell types (Bumsted et al., 1997; Bumsted & Hendrickson, 1999; Xiao & Hendrickson, 2000). However, L and M cones appear to represent a single cell type for which the final identity as an L versus M cone is simply determined by the opsin gene that is expressed (Nathans, 1999; Wang et al., 1999; Smallwood et al., 2002). An enhancer that has been termed the locus control region (LCR) is shared by the L and M genes and is required for normal opsin gene expression (Nathans et al., 1989; Wang et al., 1992). Nathans et al. (1989) have proposed that the LCR binds to an L or M gene promoter by an entirely random process; however, the observed foveal-to-peripheral gradient of increasing L:M ratio represents a non-random feature of opsin gene expression. This gradient parallels central to peripheral developmental processes (LaVail et al., 1991; Bumsted et al., 1997; Martin et al., 2000; Xiao & Hendrickson, 2000). Chromatin remodeling is associated with differentiation and controls activation and silencing of gene expression in an ongoing, dynamic process that occurs before and after cells undergo their final cell division (Ringrose & Paro, 2004). Chromatin modifications are transmitted through mitosis from mother to daughter cell as a record of its transcriptional history. Daughter cells can change the epigenetic chromatin marks; however, this capacity diminishes as development progresses, until ultimately each cell is locked into a specific pattern of gene expression. Cells at the retinal periphery that are born late relative to cells in the fovea have been through more mitoses and they have accumulated strong epigenetic chromatin marks representing their transcriptional history.

There is evidence that chromatin remodeling is an important component of L versus M cone differentiation (Knoblauch et al., 2006; Neitz et al., 2006; McMahon et al., 2008; Gunther et al., 2008). We propose that during gestation both L and M genes are active in each cone and the cell cycles randomly between transcription of either L or M opsin. However, before birth, as the retina develops there are two competing processes. One is chromatin remodeling, which decreases the probability an opsin will be transcribed in future cycles. The other is transcription of a particular gene during a cycle, which protects it from being subjected to remodeling thus increasing the probability of transcription in future cycles. Over the long run, in every cell as the competition plays out, one gene remains actively transcribed while any other genes in the X-chromosome array are permanently silenced fixing the identity of a cone for its lifetime. This process explains the increase in L:M cone ratio in the periphery. If the regulatory sequences of the M genes are slightly more prone to chromatin remodeling and gene silencing, with progressing eccentricity cells will have passed through growing numbers of cell divisions increasingly lowering the probability that an M gene will be the one to remain active. Thus, it appears that most people are effectively deuteranopes in the far periphery.

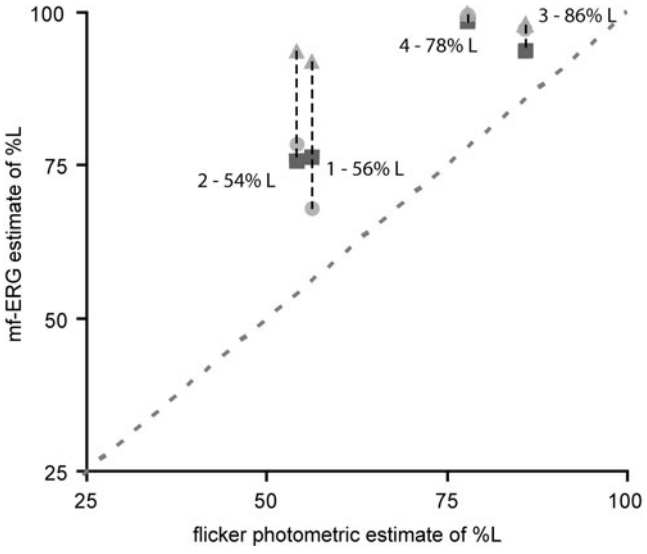

Fig. 3. L and M cone contributions to flicker ERG obtained using conventional ERG flicker photometry verses those obtained using the wide-field mf-ERG. Different symbols represent different eccentricities; diamonds, ring 2; filled circles, ring 3; triangles, ring 4. Foveal cone ratios estimated from conventional flicker photometric ERGs correlate well with inner rings from mf-ERG, however, in the far periphery all subjects approach 100% contribution from L cones.

Acknowledgments

We thank J. Pokorny for his help with the design of the PFM circuit. This work was supported by National Institutes of Health grants EY09303, EY09620, a Core Grant for Vision Research EY01981, Research to Prevent Blindness, the GAANN Fellowship, and the David and Ruth S. Coleman Charitable Foundation.

References

Albrecht, J., Jägle, H., Hood, D.C. & Sharpe, L.T. (2002). The multifocal electroretinogram (mfERG) and cone isolating stimuli: Variation in L- and M-cone driven signals across the retina. *Journal of Vision* **2**, 543–558.

Bollinger, K., Sjoberg, S., Neitz, M. & Neitz, J. (2004). Topographical cone photopigment gene expression in deutan-type red-green color vision defects. *Vision Research* **34**, 135–145.

Bowmaker, J.K., Parry, J.W.L. & Mollon, J.D. (2003). The arrangement of L and M cones in human and a primate retina. In *Normal and Defective Colour Vision*, ed. Mollon, J.D., Pokorny, J. & Knoblauch, K., pp. 39–50. New York: Oxford University Press.

Bumsted, K. & Hendrickson, A. (1999). Distribution and development of short-wavelength cones differ between Macaca monkey and human fovea. *Journal of Comparative Neurology* **403**, 502–516.

Bumsted, K., Jasoni, C., Szel, A. & Hendrickson, A. (1997). Spatial and temporal expression of cone opsins during monkey retinal development. *Journal of Comparative Neurology* **378**, 117–134.

Carroll, J., McMahon, C., Neitz, M. & Neitz, J. (2000). Flicker-photometric electroretinogram estimates of L:M cone photoreceptor ratio in men with photopigment spectra derived from genetics. *Journal of the Optical Society of America A-Optics Image Science and Vision* **17**, 499–509.

Carroll, J., Neitz, M. & Neitz, J. (2002). Estimates of L:M cone ratio from ERG flicker photometry and genetics. *Journal of Vision* **2**, 531–542.

Deeb, S.S., Diller, L.C., Williams, D.R. & Dacey, D.M. (2000). Interindividual and topographical variation of L:M cone ratios in monkey retinas. *Journal of the Optical Society of America A* **17**, 538–544.

Gunther, K.L., Neitz, J. & Neitz, M. (2008). Nucleotide polymorphisms upstream of the X-chromosome opsin gene array tune L:M cone ratio. *Visual Neuroscience* **this issue**.

Hagstrom, S.A., Neitz, J. & Neitz, M. (1998). Variations in cone populations for red-green color vision examined by analysis of mRNA. *NeuroReport* **9**, 1963–1967.

Hagstrom, S.A., Neitz, M. & Neitz, J. (2000). Cone pigment gene expression in individual photoreceptors and the chromatic topography of the retina. *Journal of the Optical Society of America A-Optics Image Science and Vision* **17**, 527–537.

Hofer, H., Carroll, J., Neitz, J., Neitz, M. & Williams, D.R. (2005). Organization of the human trichromatic cone mosaic. *Journal of Neuroscience* **25**, 9669–9679.

Hood, D.C., Yu, A.L., Zhang, X., Albrecht, J., Jägle, H. & Sharpe, L.T. (2002). The multifocal visual evoked potential and cone-isolating stimuli: Implications for L- to M-cone ratios and normalization. *Journal of Vision* **2**, 178–189.

Jacobs, G.H., Neitz, J. & Krogh, K. (1996). Electroretinogram flicker photometry and its applications. *Journal of the Optical Society of America* **13**, 641–648.

Knoblauch, J., Neitz, M. & Neitz, J. (2006). An urn model of the development of L/M cone ratios in human and macaque retina. *Visual Neuroscience* **23**, 591–596.

Kremers, J., Stepien, M.W., Scholl, H.P. & Saito, C. (2003). Cone selective adaptation influences L- and M-cone driven signals in electroretinography and psychophysics. *Journal of Vision* **3**, 146–160.

LaVail, M.M., Rapaport, D.H. & Rakic, P. (1991). Cytogenesis in the monkey retina. *Journal of Comparative Neurology* **309**, 86–114.

Lindenberg, T., Horn, F.K. & Korth, M. (2003). Cyclic summation versus m-sequence technique in the multifocal ERG. *Graefes Arch Clin Exp Ophthalmol* **241**, 505–510.

Martin, P.R., Grunert, U., Chan, T.L. & Bumsted, K. (2000). Spatial order in short-wavelength-sensitive cone photoreceptors: A comparative study of the primate retina. *Journal of the Optical Society of America* **17**, 557–579.

McMahon, C., Carroll, J., Awua, S., Neitz, J. & Neitz, M. (2008). The L:M cone ratio in males of African descent with normal color vision. *Journal of Vision* **8**, 1–9

Murray, I.J., Parry, N.R., Kremers, J., Stepien, M. & Schild, A. (2004). Photoreceptor topography and cone-specific electroretinograms. *Visual Neuroscience* **21**, 231–235.

Nathans, J. (1999). The evolution and physiology of human color vision: Insights from molecular genetic studies of visual pigments. *Neuron* **24**, 299–312.

Nathans, J., Davenport, C.M., Maumenee, I.H., Lewis, R.A., Hejtmancik, J.F., Litt, M., Lovrien, E., Weleber, R., Bachynski, B., Zwas, F., Klingaman, R. & Fishman, G. (1989). Molecular genetics of blue cone monochromacy. *Science* **245**, 831–838.

Neitz, M., Balding, S.D., McMahon, C., Sjoberg, S.A. & Neitz, J. (2006). Topography of long- and middle-wavelength sensitive cone opsin gene expression in human and Old World monkey retina. *Visual Neuroscience* **23**, 379–385.

Ringrose, L. & Paro, R. (2004). Epigenetic regulation of cellular memory by the Polycomb and Trithorax group proteins. *Annual Review Genetics* **38**, 413–443.

Roorda, A., Metha, A., Lennie, P. & Williams, D.R. (2001). Packing arrangement of the three cone classes in primate retina. *Vision Research* **41**, 1291–1306.

Roorda, A. & Williams, D.R. (1999). The arrangement of the three cone classes in the living human eye. *Nature* **397**, 520–522.

Smallwood, P.M., Wang, Y. & Nathans, J. (2002). Role of a locus control region in the mutually exclusive expression of human red and green cone pigment genes. *Proceedings of the National Academy of Sciences USA* **99**, 1008–1011.

Swanson, W.H., Ueno, T., Smith, V.C. & Pokorny, J. (1987). Temporal modulation sensitivity and pulse-detection thresholds for chromatic and luminance perturbations. *Journal of the Optical Society of America* **4**, 13.

Valeton, J.M. (1983). Photoreceptor light adaptation models: An evaluation. *Vision Research* **23**, 1549–1554.

Valeton, J.M. & van Norren, D. (1983). Light adaptation of primate cones: An analysis based on extracellular data. *Vision Research* **23**, 1539–1547.

Wang, Y., Macke, J.P., Merbs, S.L., Zack, D.J., Klaunberg, B., Bennett, J., Gearhart, J. & Nathans, J. (1992). A locus control region adjacent to the human red and green visual pigment genes. *Neuron* **9**, 429–440.

Wang, Y., Smallwood, P.M., Cowan, M., Blesh, D., Lawler, A. & Nathans, J. (1999). Mutually exclusive expression of human red and green visual pigment-reporter transgenes occurs at high frequency in murine cone photoreceptors. *Proceedings of the National Academy of Sciences USA* **96**, 5251–5256.

Xiao, M. & Hendrickson, A. (2000). Spatial and temporal expression of short, long/medium or both opsins in human fetal cones. *Journal of Comparative Neurology* **425**, 545–559.